



LAWRENCE
LIVERMORE
NATIONAL
LABORATORY

Coupled--Channels Effects In Optical Potentials For Deformed Nuclei

I. J. Thompson, F. S. Dietrich, W. E. Ormand

December 20, 2013

NEMEA-7/CIELO International Collaboration on Nuclear Data
Geel, Belgium
November 5, 2013 through November 8, 2013

Disclaimer

This document was prepared as an account of work sponsored by an agency of the United States government. Neither the United States government nor Lawrence Livermore National Security, LLC, nor any of their employees makes any warranty, expressed or implied, or assumes any legal liability or responsibility for the accuracy, completeness, or usefulness of any information, apparatus, product, or process disclosed, or represents that its use would not infringe privately owned rights. Reference herein to any specific commercial product, process, or service by trade name, trademark, manufacturer, or otherwise does not necessarily constitute or imply its endorsement, recommendation, or favoring by the United States government or Lawrence Livermore National Security, LLC. The views and opinions of authors expressed herein do not necessarily state or reflect those of the United States government or Lawrence Livermore National Security, LLC, and shall not be used for advertising or product endorsement purposes.

Coupled-channels effects in optical potentials for deformed nuclei

I.J. Thompson, F.S. Dietrich and W.E. Ormand,
Lawrence Livermore National Laboratory L-414, Livermore, CA 94551, USA

Abstract

Coupled-channels calculations for neutron scattering on actinide nuclei have recently been shown to need more excited states for convergence than was previously believed. The poor convergence shows up especially when calculating the total and the compound-nucleus production cross sections below 1 or 2 MeV incident neutron energy. Since it is exactly the compound-nucleus production cross sections which enter into Hauser-Feshbach models for many applications, we find that previous optical potentials of Soukhovitskii and of Dietrich (FLAP2.2) are not sufficiently converged. We report on using a modified version of the Koning and Delaroche optical potential as a bare potential within coupled channels calculations. Changes to the surface imaginary strength and its diffuseness are sufficient to give competitive fits to ^{232}Th and ^{238}U total, elastic and inelastic cross sections. There remain systematic reductions in the compound-nucleus production cross section compared with Soukhovitskii (2004), indicating that further work is needed to properly extract the compound-nucleus production cross sections and their uncertainties.

Introduction

In many nuclear applications we want the cross sections for the production of compound-nucleus (CN) states when neutrons are incident on rotational nuclei. This cross section, also known as the fusion or absorption cross section, is needed for the rotational nuclei which are particularly common in the rare earth and actinide regions, as it enters into Hauser-Feshbach models for many applications. In some hot astrophysical environments we also need the equivalent cross sections for nuclei in initial excited states. We have recently (Dietrich *et al*, 2012) investigated the coupled channels calculation of these cross sections. The results of these investigations require us to reassess the extraction of optical potentials from fitting scattering data. Here we focus on neutrons + ^{238}U scattering, with the longer-term aim of generating a regional optical potential for actinide nuclei, all of which have large static deformations.

Convergence issues for rotational nuclei

Coupled-channels calculations for neutron scattering on actinide nuclei found to need more excited states for convergence than was previously believed (Dietrich *et al*, 2012). The poor convergence shows up especially when calculating the total and the compound-nucleus production cross sections below 1 or 2 MeV incident neutron energy. We first discovered this when trying to predict the CN cross sections (σ_{CN}) for neutrons incident on excited states in ^{239}Pu , following the earlier results in Kawano (2009). We found the ratios of excited-state to ground-state cross sections shown in Figure 1, and were astonished by the large fluctuations of the results with increasing the number s of levels in the coupled channels sets. We define s by $s=3$ for the ground state and two excited states, for example. Calculations with $s=3$ (commonly used in applications!) give this ratio nearly to 2.0 (Figure 1, left side), whereas converged results (Figure 1, right side) differ from unity only by 0.03%.

We conclude in general that even-even nuclei (in their $K=0$ bands) need coupled-channels sets of $s=6$ levels, whereas even-odd nuclei (with half-integer K bands) require up to 12 levels for accuracy. This is particularly critical in the fast-neutron energy range between 0.1 and 1 MeV incident energy.

Validity of the adiabatic limit, and validity of the ‘fictitious even-even model’.

The adiabatic limit is to set to zero the excitation energies E^* for all the states in a rotational band: $E^*=0$. This is equivalent to having a large (infinite actually) moment of inertia of target, or, equivalently, that the target then does not rotate during the neutron scattering time. (Dietrich *et al*, 2012) proved that then the σ_{CN} is the average

over all nuclear orientations of the CN production for each orientation, and that this applies for all nuclei (even or odd; any K).

Our numerical tests show that the adiabatic approximation is rather accurate, and moreover still at neutron energies much less than the typically excited inelastic energies. Figure 2 shows that deviations from adiabaticity in the total and elastic cross sections are at most 0.4%, for both ^{238}U and ^{235}U . The exceptionally small values of these (converged!) deviations imply a good validity of spectator approximation for target spins. The compound-nucleus production is then independent of both ground state spin I and of band-head projection K .

Furthermore, we can predict any transition $I \rightarrow I'$ from knowing all $0 \rightarrow L$ transitions. Barrett (1964) developed the partial-wave theory for adiabatic scattering on axially-symmetric deformed nuclei. From his equation (15) we can prove that the scattering amplitude $f_{I'M':IM}^K(\theta)$ for an arbitrary transition in a rotational band with band-head projection K is simply given in terms of the scattering amplitudes $f_{I'M':00}^0(\theta)$ from the (possibly fictitious) even-even nucleus with the same physical potentials and deformations:

$$f_{I'M':IM}^K(\theta) = \sum_L \langle IK, L0 | I'K \rangle \langle IM, L M' - M | I'M' \rangle f_{I'M'-M:00}^0(\theta)$$

From this result we can then easily derive the relation between the cross sections:

$$\frac{d\sigma(I \rightarrow I')}{d\Omega} = \sum_L |\langle IK, L0 | I'K \rangle|^2 \frac{d\sigma(0 \rightarrow L)}{d\Omega}$$

that was given in Lagrange (1982) but without proof. Furthermore, it is now accurate to average transmission coefficients over target spins (with m -state-count weighting), as is already commonly done in applications.

Previously used rotational models and optical potentials for neutrons

In the widely-used Hauser-Feshbach code TALYS (Koning, 2011), the default calculations are $\text{maxrot}=2$. This input parameter is the number of levels in addition to the ground state ($s=\text{maxrot}+1$), making $s=3$. The FLAP2.2 actinide potential was fitted with $s=3$. Comparing these numbers with our convergence conclusions above indicates a clear need to re-run practical calculations, and *also* re-evaluate the fitting of the optical potentials themselves.

The Soukhovitskii *et al* (2004) optical potential has been a standard for actinide potentials for many purposes. They fitted their potentials using what they called ‘saturated coupling’ of $\text{maxrot}=4$ ($s=5$). These $s=5$ calculations are indeed converged for most observables: mainly σ_{TOT} , $\sigma_{\text{el}}(\theta)$, and $\sigma_{\text{inel}}(\theta)$. *However*, as we see in Figure 3, they are *not* fully converged for absorption (the CN-production cross section σ_{CN}). Recent improvements to the Soukhovitskii (2004) potential have included satisfying dispersion relations (Capote, 2008), including off-diagonal isospin terms (Quesada, 2007), and including additional side bands (Quesada, 2013), but the differences in the CN cross sections between $s=5$ and $s=7$ calculations still remain (Capote, *private communication*). The combination of all these facts shows the need for a general reexamination the determination of CN cross section on the basis of other experimental scattering observables.

A new optical potential fit for actinide nuclei

We have therefore sought to improve the FLAP 2.2 regional actinide optical potential from Frank Dietrich (Escher, 2010), where the potential parameters are piecewise-linear functions of neutron energy. Soukhovitskii (2004) used analytic functions for his energy dependence, but these are not so easy to adjust in the various energy regions. In order to have a fitted optical potential that is suitably independent of those two potentials, after some trials we found it satisfactory to use a modified version of the Koning and Delaroche optical potential (Koning, 2003). That potential was fitted to mainly spherical nuclei of mass numbers below $A=209$, so some changes must be expected when that global form is extrapolated up to $A=232-242$, and also when it becomes a bare potential within a coupled-channels set.

We therefore start with a deformed Koning-Delaroche global potential, as does Nobre (2013) for rare earth targets. Our research showed that small changes to the surface imaginary strength and its diffuseness are sufficient to give competitive fits to ^{232}Th and ^{238}U total, elastic and inelastic cross sections. The first task is to fit ^{238}U , the results for which we show in this proceedings. Further reports will examine the fits for ^{232}Th , and then other actinides. The result we call the ‘FLAP 3.0’ parameter set.

In the following Figures 4 through 7 showing neutron+²³⁸U scattering, the blue line is Soukhovitskii (2004), and the green line is also Soukhovitskii (2004) but with Koning's (2003) simplified formula for Fermi energies. We use rotational deformations $\beta_2=0.223$, $\beta_4=0.056$. The red lines are our new FLAP3.0, using $\beta_2=0.213$, $\beta_4=0.043$ from a re-analysis of inelastic cross sections. The two Soukhovitskii curves need to be shown, because our desire for keeping the same piecewise linear parameters for all actinides means that we need a simplified treatment of the low-energy cutoff of the imaginary potential. The absorptive part is designed to go to zero quadratically as the scattering energy approaches the Fermi energy.

Figure 4 shows the elastic angular distribution for neutrons scattered from ²³⁸U at 14.2 MeV, and Figure 5 shows the similar elastic distributions for a range of incident neutron energies from 4.5 to 10 MeV. At all energies the new FLAP 3.0 scattering distributions are as good as those from the Soukhovitskii (2004) potential, or better. Figure 6 shows on top the total cross sections, and below the CN-production cross sections. There is still a possible shortcoming in our FLAP 3.0 potential for scattering between 3 and 6 MeV, as this energy range has proved to be recalcitrant in our attempts to improve the fit to the data.

What is most interesting are systematic reductions in the lower-left plot in Figure 6 for the compound-nucleus production cross section compared with Soukhovitskii in the energy range 0.06 to 2 MeV. This discrepancy arises apparently because of multiple minima in the goodness-of-fit when searching for parameters, and has been found only because we use a parameter search that is essentially independent of that leading to the Soukhovitskii (2004) parameterization. This discrepancy indicates definitively that further work is needed to properly determine the uncertainties of the extracted compound-nucleus production cross sections, and thus to see exactly how well they are in fact constrained by presently available scattering data.

Figure 7 shows the fitting of the low-energy neutron resonance parameters: the *s*- and *p*-wave strength functions S_0 and S_1 , as well as the 'potential scattering radius' R' . We can see the effects of the different treatments in the blue-line and green-line treatments of the Soukhovitskii cutoff of the imaginary potential at low energies. The Fermi energy in the blue symbols gives a significantly better fit to the *s*-wave S_0 parameter. This difference can be seen also in the lower left plot of Figure 6, with the different trends of the CN cross section below 0.03 MeV neutron scattering energy.

Conclusions

We need to pay good attention to the convergence of inelastic scattering in rotational models. We bring to general attention the considerable uncertainties in extraction of CN-production cross sections from other observables. To help in this program of research, we have developed and presented a new actinide potential (FLAP 3.0) that is independent of the fit of Soukhovitskii (2004). Furthermore, when using the new potentials, we may well benefit from the good physical accuracy of adiabatic model for rotational excitations, as well as from the use of 'fictitious even-even model' when faced with the onerous numerical task of calculating rotational excitation cross sections for odd nuclei with over 12 levels constituting the coupled channels set, as needed for converged results.

Acknowledgements

This work was performed under the auspices of the U.S. Department of Energy by Lawrence Livermore National Laboratory under Contract DE-AC52-07NA27344.

References

- [1] W.P. Abfalterer, F.B. Bateman, F.S. Dietrich, R.W. Finlay, R.C. Haight and G.L. Morgan, Phys. Rev. C **63**, 044608 (2001).
- [2] R.C. Barrett, Nucl. Phys. **51**, 27 (1964)
- [3] R. Capote, S. Chiba, E.S. Soukhovitskii, J.M. Quesada and E. Bauge, J. Nucl. Sci. Tech. **45**, 333 (2008)
- [4] F.S. Dietrich, T. Kawano and I.J. Thompson, Phys. Rev. C **85**, 044611 (2012)
- [5] J. E. Escher and F.S. Dietrich, Phys. Rev. C **81**, 024612 (2010). [FLAP 2.2 in Appendix A].
- [6] A.J. Koning and J.-P. Delaroche, Nucl. Phys. A **713**, 231 (2003).
- [7] A.J. Koning, S. Hilaire and M.C. Duijvestijn, TALYS 1.4 (2011), URL; www.talys.eu

- [8] S. Guanran, H. Tangzi, W. Shenlin, Y. Chunying, Li Anli, T. Hongqing, S. Qingbiao, Z. Zhixiang and G. Fuhua, Chinese J. Nucl. Phys. **6**, 193 (1984)
- [9] T. Kawano, P. Talou, J. E. Lynn, M. B. Chadwick, and D. G. Madland, Phys. Rev. C **80**, 024611 (2009).
- [10] L. F. Hansen, A.B. Pohl, C. Wong, R.C. Haight and Ch. Lagrange, Phys. Rev. C **34**, 2075 (1986).
- [11] Ch. Lagrange, O. Bersillon, and D. G. Madland, Nucl. Sci. Eng. **83**, 396 (1983)
- [12] S. F. Mughabghab. Atlas of Neutron Resonances, 5th edition, Elsevier: Amsterdam (2006).
- [13] G.P.A. Nobre, F.S. Dietrich, M. Herman, A. Palumbo, S. Hoblit and D. Brown, arXiv:1311.1735 [nucl-th] (2013).
- [14] W.P. Poenitz, J.F. Whalen and A.B. Smith, Nucl. Sci. Eng. **78**, 333 (1981)
- [15] W.P. Poenitz and J.F. Whalen, Argonne Report ANL/NDM-80 (May, 1983)
- [16] J.M. Quesada, R. Capote, E.S. Soukhovitskii and S. Chiba, Phys. Rev. C **76**, 057602 (2007).
- [17] J.M. Quesada, E.S. Soukhovitskii, R. Capote and S. Chiba, EPJ Web of Conferences **42**, 02005 (2013)
- [18] A. B. Smith and S. Chiba, Ann. Nucl. Energy **23**, 459 (1996)
- [19] E. S. Soukhovitskii, S. Chiba, J.Y. Lee, O. Iwamoto and T. Fukahori, J. Phys. G **30**, 904(2004)

Figure 1. Ratio of CN cross sections for initial excited to initial ground states, with neutrons incident on ^{239}Pu . The lines are for different sizes of coupled-channels sets. The right figure is an enlargement for 11 to 15 coupled levels.

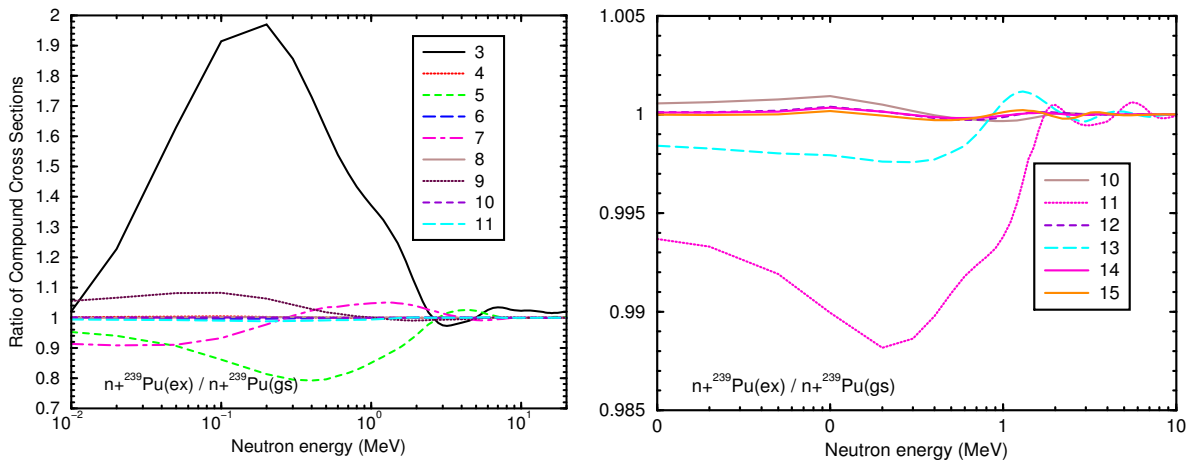


Figure 2. For total (left) and CN cross sections (right), the ration of non-adiabatic to adiabatic scattering of neutrons on ^{235}U (red lines) and ^{238}U (blue lines).

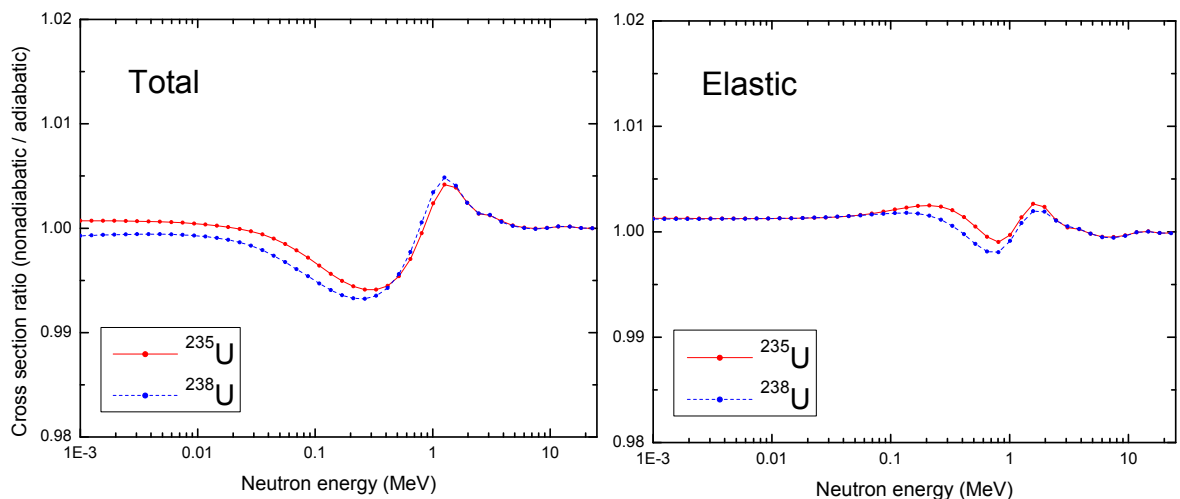


Figure 3. Compound-nucleus production cross sections for neutrons incident on ^{238}U , using the Soukhovitskii (2004) potential with different numbers of levels included in the coupled channel set.

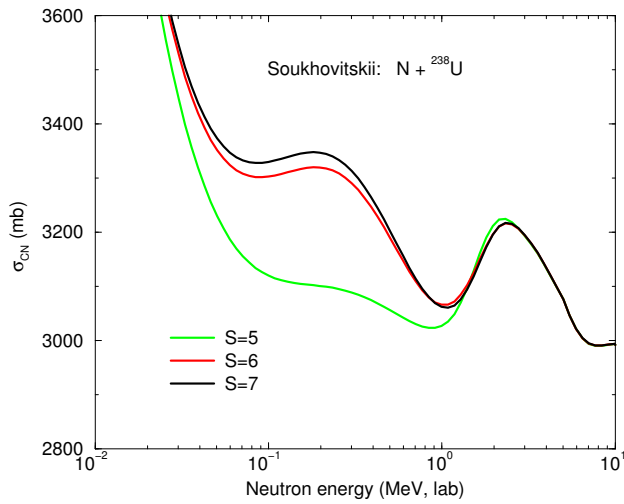


Figure 4. Elastic scattering angular distributions of neutrons on ^{238}U at 14.2 MeV incident energy. The blue and green curves use the Soukhovitskii optical potential as explained in the text, and the red curve is the new FLAP3.0 fit. The data are from Guanran (1984) and Hansen (1986).

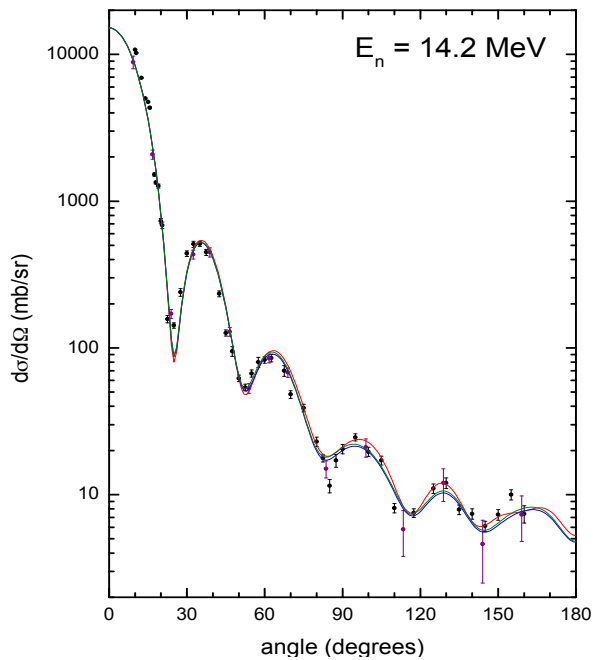


Figure 1. Elastic scattering for $n + {}^{238}\text{U}$ at incident energies from 4.5 to 10 MeV. The lines have the same significance as in the previous figure. The data are from Smith (1996).

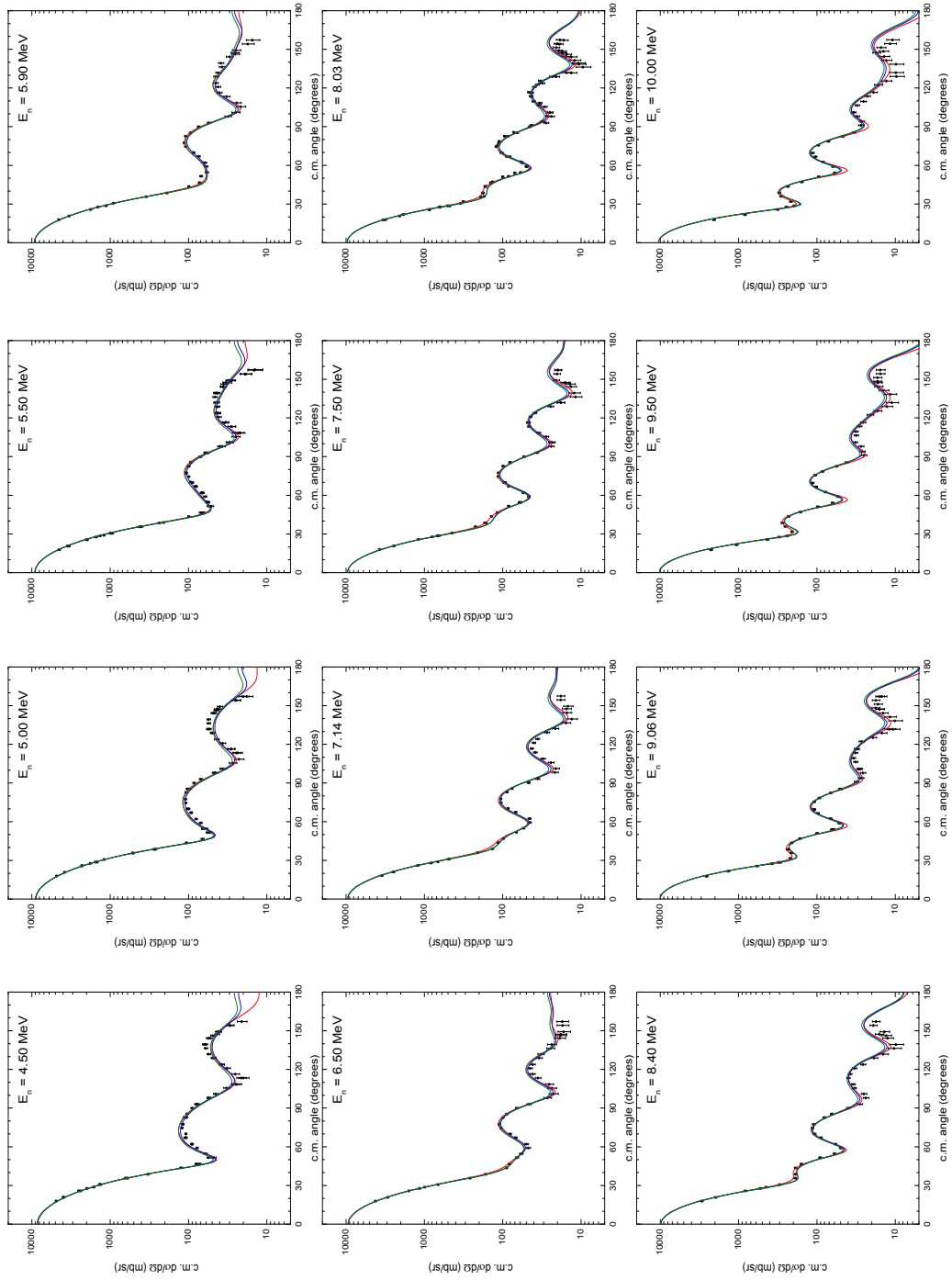


Figure 6. Total (upper) and CN-production (lower) cross sections for $n + {}^{238}\text{U}$ scattering. The left plots show 0.01 to 10 MeV, whereas the right plots show the results for incident energies from 1 to 200 MeV with an expanded vertical scale. The data are from Poenitz (1981,1983) and Abfalterer (2001).

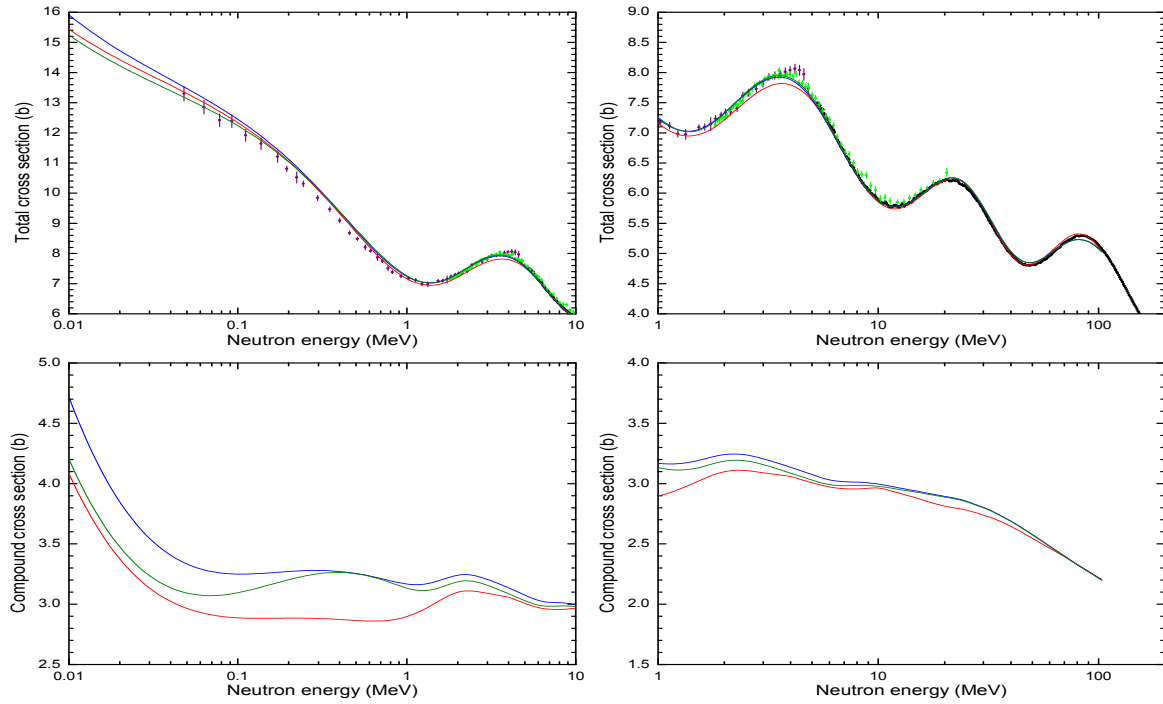


Figure 7. Neutron strength functions describing low-energy $n + {}^{238}\text{U}$ scattering. S_0 and S_1 are (respectively) the s- and p-wave strength functions, and R' is the potential scattering radius. The data are from Mughabghab (2006)

